# A single in vivo-selected point mutation in the active center of *Toxoplasma gondii* ferredoxin-NADP$^+$ reductase leads to an inactive enzyme with greatly enhanced affinity for ferredoxin

Nadine Thomsen-Zieger[a], Vittorio Pandini[b], Gianluca Caprini[b], Alessandro Aliverti[b], Jörg Cramer[c], Paul M. Selzer[c], Giuliana Zanetti[b], Frank Seeber[a,*]

[a]*FB Biologie/Parasitologie, Philipps-Universität Marburg, Karl-von-Frisch-Str., D-35032 Marburg, Germany*
[b]*Dipartimento di Scienze Biomolecolari e Biotecnologie, Università degli Studi di Milano, Via Celoria 26, 20133 Milano, Italy*
[c]*Intervet Innovation GmbH, BioChemInformatics, Zur Propstei, D-55270 Schwabenheim, Germany*

Received 16 August 2004; accepted 9 September 2004

Available online 28 September 2004

Edited by Hans Eklund

**Abstract Electron transfer between plant-type [2Fe–2S] ferredoxin (Fd) and ferredoxin-NADP$^+$ reductase (FNR) depends on the physical interaction between both proteins. We have applied a random mutagenesis approach with subsequent in vivo selection using the yeast two-hybrid system to obtain mutants of *Toxoplasma gondii* FNR with higher affinity for Fd. One mutant showed a 10-fold enhanced binding using affinity chromatography on immobilized Fd. A single serine-to-arginine exchange in the active site was responsible for its increased affinity. The mutant reductase was also enzymatically inactive. Homology modeling of the mutant FNR–Fd complex predicts substantial alterations of protein–FAD interactions in the active site of the enzyme with subsequent structural changes. Collectively, for the first time a point mutation in this important class of enzymes is described which leads to greatly enhanced affinity for its protein ligand.**


*Keywords:* Apicomplexa; Apicoplast; Ferredoxin NADP$^+$ reductase; Affinity mutant; Two-hybrid system

## 1. Introduction

Ferredoxin-NADP$^+$ reductases (EC 1.18.1.2, FNR) represent a functional class of flavin oxidoreductases found in prokaryotes, mitochondria of eukaryotes and plastids of plants where they fulfill a variety of metabolically important tasks. In general, FNRs catalyze the exchange of reducing equivalents between NAD(P)(H) and [2Fe–2S] ferredoxins (Fds), small, single-electron carrier proteins [1,2]. In chloroplasts, this leads to the generation of NADPH (with electrons originating from photosystem I) which is then delivered to the Calvin cycle for $CO_2$ fixation [3]. In contrast, the provision of reduced Fd under consumption of NADPH is found in bacteria, mitochondria and non-photosynthetic plastids [1,4]. In the latter case, this reaction is catalyzed by distinct isoenzymes (also referred to as non-photosynthetic FNRs) with strong homology to the chloroplast and cyanobacterial FNRs [2].

We previously reported the cloning and biochemical characterization of such a non-photosynthetic plant-type FNR/Fd redox system present in a plastid-derived organelle called apicoplast of the obligate intracellular protozoan parasite *Toxoplasma gondii* and other parasites of the phylum Apicomplexa [5–7]. The apicoplast is a functional remnant of a secondary algal endosymbiont present in most apicomplexan parasites (including *Plasmodium falciparum*, the causative agent of malaria) and has been shown to be essential for their survival (for review see [8,9]). The exact function of the Fd/FNR couple in the parasite plastid is unclear at present. However, we and others have provided bioinformatic evidence that the apicoplast contains all essential components for [Fe–S] biosynthesis [10,11]. In analogy to the mitochondrion of yeast, where the mitochondrial-type FNR and Fd (also called adrenodoxin reductase and adrenodoxin, respectively) are essential for this biosynthetic pathway (reviewed in [12]), we anticipate that the apicoplast Fd/FNR redox pair fulfills a similar task in apicomplexan parasites [4]. Other target proteins for reduced Fd like fatty acid desaturase are additional candidates as electron acceptors [13].

A unique structural feature of all apicomplexan FNRs identified so far is a peptide insertion in the FAD-binding domain of variable length (10–45 aa) and sequence [5,7]. This insert extends the short loop present in other FNRs that connects two adjacent β-strands of the barrel motif. The apicomplexan insertion is expected to be in proximity of the Fd-binding site of the enzyme [7], but its influence on the binding of Fd to FNR is unknown. To better understand the protein–protein interaction between these molecules, we used a yeast two-hybrid approach to screen randomly generated *T. gondii* FNR (TgFNR) mutants for enhanced affinity to Fd. Here, we report that a single point mutation is sufficient to drastically enhance the affinity of TgFNR for Fd and that this amino acid exchange also leads to an inactive enzyme. Such a dual phenotype of the mutant would not have been anticipated per se, validating the advantage of this in vivo approach over rational design for generating such point mutations.

* Corresponding author. Fax: +49-6421-2821531.
*E-mail address:* seeber@staff.uni-marburg.de (F. Seeber).

*Abbreviations:* HA, hemaglutinin epitope tag; Fd, ferredoxin; FNR, ferredoxin-NADP$^+$ oxidoreductase; mutTgFNR, double-mutant of TgFNR; PfFd, *P. falciparum* Fd; sl spinach leaf; wt, wild-type; TgFd, *T. gondii* Fd; TgFNR, *T. gondii* FNR

0014-5793/$22.00 
doi:10.1016/j.febslet.2004.09.042

## 2. Materials and methods

### 2.1. In vivo selection of high-affinity TgFNR mutant

Generation of random point mutations in yeast by mutagenic PCR in the presence of $Mn^{2+}$ followed by in vivo gap repair was done according to Vidal [14]. The used LexA-based yeast two-hybrid constructs and protocols have been reported [6]. The coding sequence of mature TgFNR was amplified using primers described previously [5] for 10 rounds under standard conditions before two concentrations of $MnCl_2$ (50 and 100 μM) were added into two separate tubes and further amplified for additional 30 rounds. The resulting fragments from both reactions were combined and then transformed into yeast strain EGY194 containing *P. falciparum* Fd (PfFd) cloned into pGILDA (pGILDA-PfFd) together with *Nco*I-cut pB42AD-TgFNR. TgFNR amplified under standard conditions was used as a control in a separate transformation. Transformants were then plated onto His/Trp/Leu drop-out medium (QBiogene; Heidelberg, Germany) containing 2% galactose. Under these conditions only interacting colonies should be able to grow, and due to the lower number of lexA binding sites upstream of the Leu2 reporter gene in EGY194 only TgFNR molecules with a higher affinity for Fd compared to wtTgFNR should be able to grow within 3–5 days [15]. From 26 potentially faster growing colonies, one was selected which gave consistently higher cell mass and stronger beta-galactosidase activity during initial characterization. Its FNR coding sequence was therefore fully sequenced and found to contain five point mutations (double-mutant of TgFNR, mutTgFNR).

### 2.2. Site-directed mutagenesis of mutTgFNR

For reversion of pS1 and pB42AD containing mutTgFNR to the individual single point mutants shown in Fig. 2, the QuikChange XL site-directed mutagenesis kit (Stratagene) was used according to the manufacturer's instructions. To facilitate verification of correct clones, a diagnostic *Bsr*DI, *Bsa*WI or *Bst*YI restriction site, respectively, was introduced into the respective mutagenic primer without changing the coding sequence [16]. The mutagenic primers were as follows: S267V sense, CAAAGAAATTCCGTTCAACCGGACGGGCAAGGACAGC; S267V antisense, CCATCCCGGCTGGACGCAATGACGTATATCCGCGGAAGC; R242Q sense, CAAAGAAATTCCGTTCAACCGGACGGGCAAGGACAGC; R242Q antisense, GCTGTCCTTGCCCGTCCGGTTGAACGGAATTTCTTTG; R267S sense, GCTTCCGCGGATATACAGCATTGCGTCCAGCCGGGATG; R267S antisense, CATCCCGGCTGGACGCAATGCTGTATATCCGCGGAAGC. All selected clones were verified by sequencing.

### 2.3. SDS–PAGE and immunoblot analysis

Yeast cells were grown in the presence of 2% galactose for 6 h and extracts were then generated using glass beads and cracking buffer (5% SDS, 8 M urea, 40 mM Tris–HCl, pH 6.8, 0.1 mM EDTA, 1% 2-mercaptoethanol, 0.4 mg/ml bromophenol blue). SDS–PAGE and immunoblot analysis were performed as described previously [5]. Anti-hemaglutinin epitope tag (anti-HA) rat monoclonal antibody (Roche; diluted 1:1000) was used to detect HA-tagged proteins on blots.

### 2.4. Overproduction and purification of TgFNR mutants

*Escherichia coli* RRIΔM15 cells transformed with expression plasmids (pS1-S/TgFNR and those carrying the mutations in the TgFNR sequence) were grown at 30 °C as described for wtTgFNR [6]. Purification of the three mutants was performed as reported for the wild-type (wt) enzyme, omitting the final step on SP-Sepharose [6]. After gel filtration on a PD10 column (Amersham Biosciences) in 150 mM Tris–HCl, pH 7.0, containing 10% glycerol, 1 mM EDTA, and 1 mM dithiothreitol, the enzymes were stored at −20 °C.

### 2.5. Protein characterization methods

Absorption spectra, determination of FAD content and activity assays were carried out as described [6]. Circular dichroism spectra were recorded as described using a Jasco J810 spectropolarimeter [17]. Conjugation of highly purified *T. gondii* Fd (TgFd) to the CNBr-activated resin and affinity chromatography of the various TgFNRs were performed under the same conditions as previously reported for spinach Fd I [6]. Titrations of FNR tryptophan fluorescence have been described [18].

### 2.6. Homology modeling

Homology models of TgFNR and the TgFNR S267R mutant were calculated using the program Modeller implemented in the Insight II 2000.2 software package (Insight II Modeling Environment, Release 2000.2, Accelrys Inc., San Diego, USA). All calculations were carried out under default conditions unless otherwise stated. To build the homology models, five FNR crystal structures were used as template proteins: PDB entries 1GO2, 1QUE (*Anabaena* sp.), 1GAW, 1GAQ (*Zea mays*) and 1FND (*Spinacia oleracea*). For sequence alignments, the PAM 250 matrix within the Insight II multisequence alignment tool was used. For the alignment of wtTgFNR and TgFNR-S267R to the pre-aligned templates, the BLOSUM 62 matrix implemented in Modeller's ALIGN123 module was taken. For each of the two sequences, four homology models were generated using the default conditions with the highest optimization level, and subsequently four additional structures were generated with a high loop refinement for each of the first four homology models. In summary, 16 homology models were built for each protein to ensure the generation of the highest possible structure quality. To determine the placement of FAD in the homology models' active sites, its potential position was investigated by superimposition of the protein model with the Fd/FNR complex structure from *Z. mays* (1GAQ). Subsequently, the active site regions of the proteins were defined to consist of all residues within a 6 Å radius around the proposed position of FAD. To investigate how single amino acid mutations at position 267 interfere with FAD and subsequently with the whole protein, FAD was re-docked into wt as well as into the mutated active sites of the protein models, keeping the protein structure rigid, using the software package GOLD 2.1 (Cambridge Crystallographic Database Center, Cambridge, UK). The homology model of TgFd was generated under the same conditions as those for TgFNR. Template Fds used were those from the green algae *Chlorella fusca* (1AWD), the cyanobacterium *Anabaena* sp. (1QT9) and from *P. falciparum* (1IUE). Visualization of the structures was done as described in [19,20].

## 3. Results and discussion

### 3.1. In vivo selection of a mutant TgFNR with enhanced affinity for Fd

Our aim was to gain insights into the interaction between TgFNR and Fd, since very little about this aspect is known in this new member of the FNR superfamily. This is in contrast to the plant Fd/FNR system where a vast number of point mutations affecting protein–protein interactions and/or enzymatic function have been characterized in the past (reviewed in [1]). Since apicomplexan and plant FNRs possess only moderate overall sequence homology [7], the approach of using random mutagenesis of TgFNR and subsequent in vivo selection rather than educated guesses based on the known structures of plant or cyanobacterial FNR was chosen. We previously described the in vivo interaction of TgFNR with Fd from both *T. gondii* and *P. falciparum* using the yeast two-hybrid system [6]. Building upon the relatively weak interaction between TgFNR and PfFd in this system, we mutagenized the coding sequence of mature TgFNR (aa 150–497) by means of random PCR mutagenesis and subsequent in vivo recombination [21] and screened for higher affinity mutants in a less sensitive yeast strain (EGY194, see Section 2 [15]). One clone consistently showed superior growth (see Fig. 1A) and high enzymatic reporter activity (data not shown) compared to non-mutagenized controls. Western blots of yeast cell extracts containing wtTgFNR and mutagenized TgFNR (mutTgFNR) grown in galactose showed faster migration of mutTgFNR (Fig. 1B), suggesting a difference in amino acid sequence between wt and mutTgFNR. Sequence analysis of mutTgFNR revealed five point mutations confined to a 126 bp region adjacent to the FAD and Fd binding sites and encompassing the

28 aa insertion [7]. Three of these mutations were translationally silent, but two resulted in two distinct amino acid changes (A to G, resulting in Q242R; A to C, resulting in S267R; Fig. 1C). While the initial screening for high affinity mutants was done with PfFd as bait, we later used Fd from *T. gondii* for all further analyses. Not very surprisingly, TgFd showed the same phenotype with mutTgFNR in the yeast two-hybrid system (see Fig. 2), owing to the high sequence similarity between these two Fds [6].

### 3.2. A single point mutation in the active center of TgFNR is responsible for enhanced affinity for Fd

To determine if both amino acid mutations were required for the apparent higher affinity to Fd, we individually back-mutated each arginine to its wt residue, giving rise to the two single mutants Q242R and S267R, respectively (Fig. 2A). Comparison of these mutants with the mutTgFNR in growth assays on leucine-deficient media revealed that the S267R mutation alone was sufficient to allow growth under selective conditions for higher affinity (Fig. 2B). A S267V mutation had no effect on Fd affinity. These results indicated that the single S267R exchange is sufficient to increase the affinity of TgFNR for apicomplexan Fds.

To confirm these results in vitro, all three mutants (mutTgFNR; TgFNR-Q242R, and TgFNR-S267R) were expressed in *E. coli* as His-tagged proteins and purified on a nickel-chelate affinity column (data not shown). Again, the double mutant migrated faster in SDS gels with respect to wtTgFNR while the single S267R mutant behaved like wt enzyme (data not shown), proving that the Q242R mutation is responsible for this behavior. Each purified enzyme was loaded at low ionic strength onto an affinity column consisting of highly purified immobilized TgFd [6] and then eluted with a linear gradient of NaCl. Elution of mutTgFNR was clearly retarded with respect to wtTgFNR (Fig. 3), indicating a stronger binding to the column and thus confirming the in vivo data. On the other hand, the S267R mutant elution profile nearly superimposed to that of the double mutant, whereas the Q242R enzyme showed an affinity for TgFd slightly lower than that of wtTgFNR (Fig. 3). When 2 M urea was present in all samples and buffers, the various enzymes were eluted at lower NaCl concentration but in the same order (data not shown), suggesting that the increased binding to TgFd is mainly due to ionic interactions.

Collectively, these data clearly demonstrate that the enhanced affinity of the double mutant for TgFd is entirely due to the change of S267 to arginine in the active center of TgFNR. This is surprising since R242, being of positive charge and therefore optimal for interaction with the negative surface of Fd [22,23], is just adjacent to the conserved active site motif RL/IYSIAS that makes extensive contact with the back (*si*-face) of the isoalloxazine ring of FAD. Also, the shorter loop that replaces the apicomplexan insertion in all other plant-type FNRs is known to be part of the Fd binding site of plant and cyanobacterial reductases [18,23–25]. Possibly, other positive residues in the TgFNR loop might be involved in some aspects of Fd binding or complex stabilization, as suggested by our homology model (Fig. 4A).

A quantitative estimate of the increase in TgFd affinity resulting from the S267R mutation was attempted by comparison with the chromatographic behavior of FNR proteins, whose $K_d$ for Fd are known [18]. MutTgFNR and TgFNR-S267R eluted with retention volumes that were increased by 19% in comparison to wtTgFNR. Under the same experi-

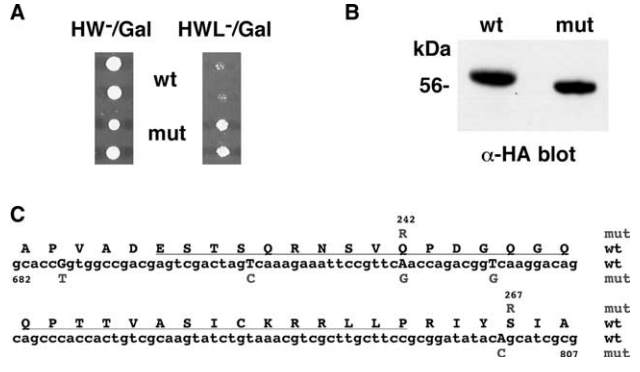


Fig. 1. Identification and characterization of a TgFNR affinity mutant. (A) Interaction of wt and mutant TgFNR with PfFd in the yeast two-hybrid system with strain EGY194. Under non-selective conditions (leucine-containing medium) no interaction is required for growth (duplicate cultures were applied), whereas on selective leucine-deficient medium only a strong interaction between the mutant FNR and PfFd leads to substantial growth. wtTgFNR grows poorly under the same conditions. (B) Electrophoretic difference of wt and mutTgFNR by 12% SDS–PAGE. Total cell lysates of yeast cells expressing wt and mutFNR, respectively, as fusion with the B42 domain of the two-hybrid vector were probed on a Western blot with an anti-HA tag antibody. The Q242R/S267R double mutant runs significantly faster than the wt protein. This difference is solely due to the Q242R mutation, since the single S267R mutant runs like wtTgFNR under these conditions (data not shown). (C) Point mutations of mutTgFNR. Shown is the DNA sequence of the respective part of mutTgFNR containing all five nucleotide changes (below DNA sequence). The resulting two amino acid changes are indicated above the DNA sequence. The underlined amino acids represent the FNR insertion of TgFNR.

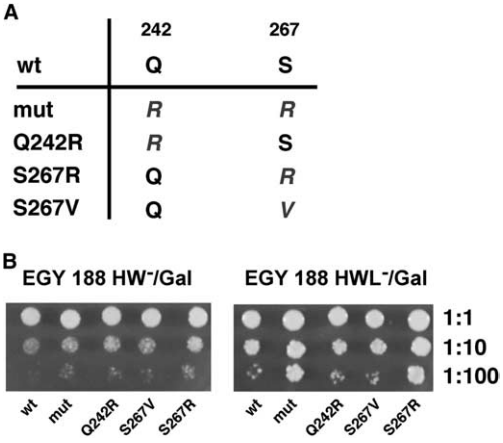


Fig. 2. Generation of individual TgFNR mutations and their influence on the interaction with Fd. (A) Amino acid changes of different FNR mutants. The wt sequence at positions 242 and 267, respectively, are shown in comparison to the double mutant (mut) and the individual single mutants discussed in the text. (B) Growth assays of yeasts expressing individual mutants of TgFNR reveal their influence on interaction with TgFd. The assay conditions are the same as in Fig. 1 except that strain EGY188 was used and TgFd served as interacting partner. Under these conditions, only mutTgFNR and the single S267R mutant show enhanced cell growth compared to wt and the other mutants. The left panel shows similar cell mass for all yeasts under non-selective control conditions. The culture plate on the right panel was incubated 24 h longer than the control plate to allow a clear distinction at the 1:100 dilution between mutTgFNR and S267R and the others.

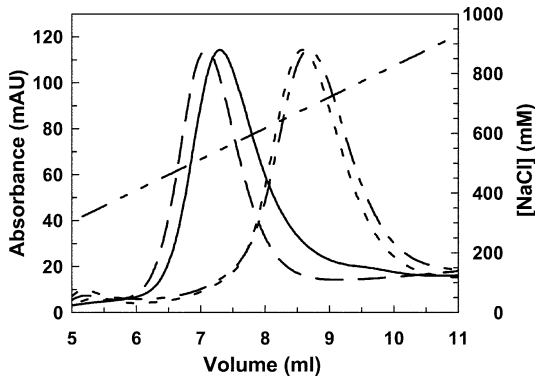


Fig. 3. Affinity chromatography of TgFNR mutant forms on a TgFd-conjugated resin. Elution profile of the different purified recombinant TgFNRs from a TgFd affinity column as a function of salt concentration is shown. Both mutTgFNR and S267R elute at higher salt concentrations, indicating tighter binding to TgFd. —, wtTgFNR; - - -, TgFNR-Q242R; ···, TgFNR-S267R; -·-, mutTgFNR; -···-, NaCl gradient.

mental conditions, the retention volume of spinach leaf (sl) FNR-K88Q [18] on a column of immobilized slFd I was decreased by 19%, as compared to wt enzyme (data not shown). Since the $K_d$ values for the complexes of the two spinach FNRs with slFd I are 110 and 10 nM, respectively [18], it is concluded that a similar alteration (~10-fold) in affinity exists for the S267R mutation and wtTgFNR, respectively. A similar estimate (~11-fold) was derived by titrating the tryptophan fluorescence of selected TgFNR forms with slFd I at low ionic strength (TgFd binds too tightly to any TgFNR form to allow the determination of its affinity constant, data not shown).

### 3.3. Catalytic activity of mutant TgFNR enzymes in vitro

Mutations of S96 of slFNR (corresponding to S267 of TgFNR) were shown previously to interfere with the proper binding of NADP(H) and subsequent hydride-transfer between the nicotinamide and isoalloxazine rings, known to be essential for enzymatic activity [17]. Activities of the mutant *T. gondii* enzymes with different electron acceptors were thus determined and compared with those of wtTgFNR (Table 1). MutTgFNR was basically inactive (1–4%) in all the reactions tested, whereas the Q242R protein was as active as the wt enzyme. The S267R mutant showed an activity level similar to that of the double mutant. Determination of the kinetic parameters of the Q242R mutant in the NADPH-ferricyanide reductase reaction yielded a slightly higher value for $k_{cat}$ ($625 \pm 6$ vs $470 \pm 9$ eq $s^{-1}$) and the same $k_m$ value for NADPH (35 μM) with respect to wtTgFNR.

Thus, as expected from our earlier work on plant FNRs, the active site mutation S267R is responsible for the lack of activity of mutTgFNR. However, in our previous study only amino acid changes of neutral charge were examined, and it could not be anticipated that changing the serine to an arginine would result in such an enhanced affinity towards Fd. Along those lines, placing a negative charge at this position in TgFNR (S267E) does not lead to a repulsion of Fd in vivo, as might be expected (data not shown). Together with other reports [26–28], these data emphasize the advantage of the two-hybrid approach in this context.

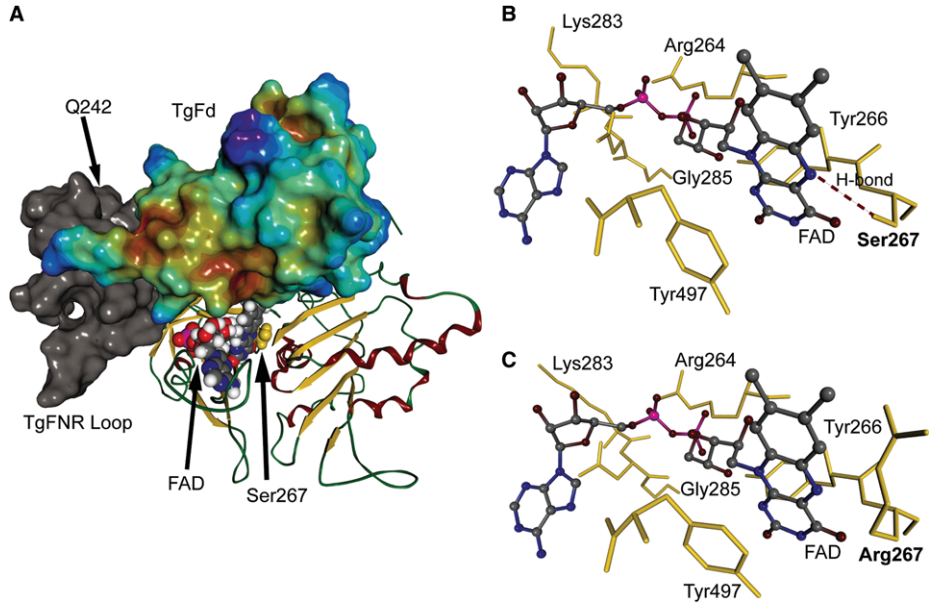


Fig. 4. Homology protein model of the *T. gondii* FNR/Fd complex. (A) wtTgFNR/TgFd complex, which was aligned based on the Fd/FNR complex of *Z. mays* (PDB 1GAQ). TgFNR is shown in a ribbon representation, whereby helices are colored in red, beta strands in yellow and loops in green, respectively. S267 is shown in yellow and the FAD molecule is displayed in CPK representation. Its position was deduced from the *Z. mays* complex. The protein loop adjacent to the active site gorge is shown with a solid gray molecular surface. TgFd is displayed in a surface representation, color-coded according to the electrostatic potential: red, negative; green, neutral; blue, positive. Note that Q242 shows no direct interaction with TgFd. (B) Detailed view of the wtTgFNR active site. The H-bond between S267 and N-5 of the isoalloxazine moiety of FAD is indicated by a dotted line. (C) Detailed view of the S267R mutation in the active site of TgFNR. In B and C, FAD is shown in ball and stick representation. Amino acids are displayed in yellow.

Table 1
Specific activities of wt and mutant TgFNRs with different electron acceptors

| TgFNR form | Activity in U/FAD (%) | | |
|---|---|---|---|
| | $K_3Fe(CN)_6$ | TgFd | slFd I |
| wtTgFNR | 21 700 ± 700 (100) | 1960 ± 6 (100) | 500 ± 2 (25) |
| TgFNR-Q242R | 23 400 ± 200 (108) | 2120 ± 6 (108) | 520 ± 1 (26) |
| TgFNR-S267R | 423 ± 30 (2) | 88 ± 1 (4) | n.d. |
| mutTgFNR | 189 ± 6 (0.9) | 55 ± 1 (3) | n.d. |

n.d., Not detectable.

### 3.4. Homology modeling of wt and S267R TgFNR/Fd complexes

To get some hint as to why the single S267R mutation has such drastic and unexpected consequences on the affinity of mutTgFNR, a homology model was constructed using the parameters as detailed in Section 2. It is based on the complex of leaf Fd and FNR from *Z. mays* [24] and the recently determined X-ray structure of PfFd. The active site region around the catalytic S267 is highly conserved in all FNRs, as determined by superimposition of the protein structures investigated. In the TgFNR/Fd complex, the Fd protein is located above the active site of FNR (Fig. 4A). Our model suggests that in the wtTgFNR/Fd complex the Fd structure also interacts with parts of the insertion loop from T235 to C262 (Fig. 4A, see also Fig. 1C), although no definite structural predictions of this loop can be made since these long insertions are absent in plant FNRs. Consequently, the precise position of Q242 relative to TgFd is unclear. In contrast, the experimentally observed inactivation of TgFNR by the S267R mutation is readily explained by the model. First of all, the sterical constrain is increased by the introduction of arginine. Secondly, the electrostatic potential is changed from a polar residue to a positively charged amino acid. Finally, arginine cannot form a hydrogen bond to N5 in the isoalloxazine moiety of FAD, which is important for the coenzyme function of FAD ([17], see also Fig. 4B and C). Based on the structural analysis of the S267R mutant, the sterical and electrostatic modifications are considered to cause major effects on the FAD function as well as on the neighboring residues Y266, I268 and Y497, respectively. To confirm these observations, we re-docked FAD into the active site of wt and mutated TgFNR protein models while the protein structure was kept rigid. In the wt protein, the detected orientation of the re-docked FAD resembled the situation observed for the maize protein template. However, in the S267R mutant the FAD molecule could not be replaced in the active site as in the wt protein. The FAD structure was either placed by the docking algorithm with a 180° rotation of the isoalloxazine moiety, or in an opposite orientation of the molecule within the active site, whereby in both cases the hydride transfer reaction of NADPH to FAD would not be possible [17]. However, circular dichroism spectra show that the FAD position changes only slightly in the S267R containing mutants (data not shown). Consequently, a re-arrangement of several active site residues as well as a motion of the adjacent loop region has to be deduced from our docking results to accommodate FAD. These modifications appear to be responsible for the stronger protein–protein interaction between mutTgFNR and TgFd. Further support for an active site re-arrangement comes from additional in silico docking experiments of FAD of another modeled TgFNR active site mutant, S267V. Using X-ray crystallography, Aliverti et al. [17] reported previously that this mutation did not lead to major movements in the active site of spinach FNR. Indeed, FAD was re-docked in the expected normal orientation also in the TgFNR S267V model, validating our conclusions.

## 4. Conclusions

We have shown here that a single amino acid replacement in the FAD domain of *T. gondii* FNR, resulting in a positive charge, leads to an unexpected increase in affinity to apicomplexan Fd and at the same time to an inactive enzyme that is no longer able to provide electrons to Fd. It is anticipated that similar Ser-to-Arg mutations in other plant-type FNRs will result in a comparable phenotype. Since the Fd redox system of Apicomplexa is considered to be a valid drug target [4], our data also highlight the possibility to change the interaction of the two proteins and thus their activity through well fitting small molecules (dissociators) able to cause topographical and electrostatic changes [29].

*Acknowledgements:* We thank F. Bonomi for help in circular dichroism measurements, and R.J. Marhöfer, F. Dzierszinski, M.J. Crawford and D.S. Roos for discussions and support. This work was supported by grants from the Deutsche Forschungsgemeinschaft (Se 322/4-1) to F.S. and from Ministero dell'Istruzione, dell'Università e della Ricerca of Italy (Prin 2002) to G.Z.

## References

[1] Carrillo, N. and Ceccarelli, E.A. (2003) Eur. J. Biochem. 270, 1900–1915.
[2] Arakaki, A.K., Ceccarelli, E.A. and Carrillo, N. (1997) FASEB J. 11, 133–140.
[3] Carrillo, N. and Vallejos, R.H. (1987) in: The Light Reactions (Barber, J., Ed.), pp. 527–560, Elsevier, Amsterdam.
[4] Seeber, F., Aliverti, A. and Zanetti, G. (2004) Curr. Pharm. Design., in press.
[5] Vollmer, M., Thomsen, N., Wiek, S. and Seeber, F. (2001) J. Biol. Chem. 276, 5483–5490.
[6] Pandini, V., Caprini, G., Thomsen, N., Aliverti, A., Seeber, F. and Zanetti, G. (2002) J. Biol. Chem. 277, 48463–48471.
[7] Bednarek, A., Wiek, S., Lingelbach, K. and Seeber, F. (2003) Exp. Parasitol. 103, 68–77.
[8] Wilson, R.J. (2002) J. Mol. Biol. 319, 257–274.
[9] Foth, B.J. and McFadden, G.I. (2003) Int. Rev. Cytol. 224, 57–110.
[10] Ellis, K.E.S., Clough, B., Saldanah, J.W. and Wilson, R.J.M. (2001) Mol. Microbiol. 41, 973–981.
[11] Seeber, F. (2002) Int. J. Parasitol. 32, 1207–1217.
[12] Mühlenhoff, U. and Lill, R. (2000) Biochim. Biophys. Acta 1459, 370–382.
[13] Ralph, S.A. et al. (2004) Nature Rev. Microbiol. 2, 203–216.

[14] Vidal, M. (1997) in: The Yeast Two-hybrid System (Bartel, P.L. and Fields, S., Eds.), pp. 109–147, Oxford University Press, New York.
[15] Estojak, J., Brent, R. and Golemis, E.A. (1995) Mol. Cell. Biol. 15, 5820–5829.
[16] Turchin, A. and Lawler Jr., J.F. (1999) Biotechniques 26, 672–676.
[17] Aliverti, A., Bruns, C.M., Pandini, V.E., Karplus, P.A., Vanoni, M.A., Curti, B. and Zanetti, G. (1995) Biochemistry 34, 8371–8379.
[18] Aliverti, A., Corrado, M.E. and Zanetti, G. (1994) FEBS Lett. 343, 247–250.
[19] Brickmann, J., Exner, T.E., Keil, M. and Marhöfer, R.J. (2000) J. Mol. Mod. 6, 328–340.
[20] Brickmann, J., Exner, T.E., Keil, M., Marhöfer, R.J. and Moeckel, G. (1998) in: The Encyclopedia of Computational Chemistry (Schleyer, P., Allinger, N.L., Clark, T., Gasteiger, J., Kollman, P.A., Schaefer III, H.F. and Schreiner, P.R., Eds.), pp. 1679–1693, John Wiley & Sons, Chichester.
[21] Muhlrad, D., Hunter, R. and Parker, R. (1992) Yeast 8, 79–82.
[22] De Pascalis, A.R., Jelesarov, I., Ackermann, F., Koppenol, W.H., Hirasawa, M., Knaff, D.B. and Bosshard, H.R. (1993) Protein Sci. 2, 1126–1135.
[23] Hurley, J.K., Morales, R., Martinez-Julvez, M., Brodie, T.B., Medina, M., Gomez-Moreno, C. and Tollin, G. (2002) Biochim. Biophys. Acta 1554, 5–21.
[24] Kurisu, G., Kusunoki, M., Katoh, E., Yamazaki, T., Teshima, K., Onda, Y., Kimata-Ariga, Y. and Hase, T. (2001) Nat. Struct. Biol. 8, 117–121.
[25] Zanetti, G., Morelli, D., Ronchi, S., Negri, A., Aliverti, A. and Curti, B. (1988) Biochemistry 27, 3753–3759.
[26] Morcos, P., Thapar, N., Tusneem, N., Stacey, D. and Tamanoi, F. (1996) Mol. Cell. Biol. 16, 2496–2503.
[27] Sharma, U.K., Ravishankar, S., Shandil, R.K., Praveen, P.V. and Balganesh, T.S. (1999) J. Bacteriol. 181, 5855–5859.
[28] Wang, H., Van Den Bergh, F., Spencer, E., Wilcox, K. and Herman, T. (1997) DNA Cell. Biol. 16, 1277–1288.
[29] Gadek, T.R. and Nicholas, J.B. (2003) Biochem. Pharmacol. 65, 1–8.